



Synthesis, characterization and antimicrobial activity of the isothiocyanato Fe(III) Girard's T hydrazone complex

BOŽIDAR ČOBELJIĆ^{1#}, ANDREJ PEVEC², ZVONKO JAGLIČIĆ³,
MILICA R. MILENKOVIĆ^{1#}, IZTOK TUREL², DUŠANKA RADANOVIĆ^{4#},
MARINA MILENKOVIĆ⁵ and KATARINA ANĐELOKOVIC^{1**#}

¹Faculty of Chemistry, University of Belgrade, Studentski trg 12–16, Belgrade, Serbia,

²Faculty of Chemistry and Chemical Technology, University of Ljubljana, Večna pot 113,
1000 Ljubljana, Slovenia, ³Institute of Mathematics, Physics and Mechanics & Faculty of

Civil and Geodetic Engineering, University of Ljubljana, Jadranska 19, Ljubljana, Slovenia,

⁴Institute of Chemistry, Technology and Metallurgy, University of Belgrade, Njegoševa 12, P.
O. Box 815, 11000 Belgrade, Serbia and ⁵Faculty of Pharmacy, Department of Microbiology
and Immunology, University of Belgrade, Vojvode Stepe 450, 11221 Belgrade, Serbia

(Received 28 August, revised and accepted 19 September 2018)

Abstract: The isothiocyanato Fe(III) complex with (*E*)-*N,N,N*-trimethyl-2-oxo-
-2-(2-(1-(pyridin-2-yl)ethylidene)hydrazinyl)ethan-1-aminium was synthesized
and characterized by elemental analysis, IR spectroscopy and X-ray analysis.
The octahedral geometry of the Fe(III) complex consists of the deprotonated
form of the hydrazone ligand coordinated through the pyridine nitrogen, azo-
methine nitrogen and carbonyl oxygen atoms with three isothiocyanato ligands
in the remaining coordination places. The measured effective magnetic mom-
ent for Fe(III) complex corresponds to high spin Fe(III) ion. The hydrazone
ligand and its Fe(III) complex showed lower activity against the tested micro-
bial strains than standard antimicrobial drugs.

Keywords: hydrazone; X-ray structure, magnetic properties; pseudohalides

INTRODUCTION

Hydrazones and their metal complexes have been intensively investigated because of their structural diversity, magnetic and spectroscopic properties and possible catalytic and biological activities.¹ In some cases, low solubility of hydrazones and their metal complexes in water limits their application. The introduction of charged functional group into the hydrazone molecule could overcome this problem.² Girard's T reagent (Scheme 1, (2-hydrazinyl-2-oxoethyl)tri-
-methylammonium chloride) reacts with carbonyl compounds and forms water

* Corresponding author: E-mail kka@chem.bg.ac.rs

Serbian Chemical Society member.

<https://doi.org/10.2298/JSC180828079C>

soluble hydrazones. This property is largely used in organic and analytical chemistry for the separation of different carbonyl compounds from complex organic mixtures. The coordination properties of Girard's T reagent hydrazones are similar to those of semicarbazones and acylhydrazones obtained with the same carbonyl compounds. The Girard's T reagent hydrazones exhibit keto–enol tautomerism and can coordinate metal ions in the non-deprotonated positively charged form or deprotonated formally neutral zwitter-ionic form. The quaternary ammonium group in complexes of Girard's T reagent hydrazones improves their water solubility and has an effect on their biological activity.³ Thiocyanate is an ambidentate pseudohalide ligand, which can be coordinated through nitrogen or sulphur donor atom as monodentate or as a bridge between metal centres.⁴ In some cases, monodentately coordinated thiocyanate ligands can participate in intermolecular hydrogen bonding between metal complexes, having significant influence on their stability in the solid state.^{5,6} Schiff bases complexes containing pseudohalide ligands are of interest due to their structural diversity, and their magnetic and spectral properties, as well as their biological activity. Recently, isothiocyanato Fe(III) complexes with dihydrazone of 2,6-diacylpyridine and Girard's T reagent ($\mathbf{H}_2\mathbf{L}^1\mathbf{Cl}_2$) were synthesized.⁷ Both iron(III) complexes $[\mathbf{Fe}\mathbf{L}^1(\text{NCS})_2]\text{SCN}\cdot 2\text{H}_2\text{O}$ and $[\mathbf{Fe}\mathbf{L}^1(\text{NCS})_2]_2[\mathbf{Fe}(\text{H}_2\text{O})(\text{NCS})_5]\cdot 4\text{H}_2\text{O}$ possess the same pentagonal-bipyramidal complex cation, while the nature of their anions depends on the mole ratio of NH_4SCN and $\text{FeCl}_3\cdot 6\text{H}_2\text{O}$ used in the reaction. These complexes showed moderate activity against the tested microbial strains. Better activity was observed for the complex possessing $[\mathbf{Fe}(\text{H}_2\text{O})(\text{NCS})_5]^{2-}$. In this work, the investigation of the coordination properties of isothiocyanato metal complexes with the condensation product of 2-acetylpyridine and Girard's T reagent (\mathbf{HLCI} , (*E*)-*N,N,N*-trimethyl-2-oxo-2-(2-(1-(pyridin-2-yl)ethylidene)hydrazinyl)ethan-1-aminium chloride) were continued. The synthesis, crystal structure, and magnetic and antimicrobial properties of isothiocyanato Fe(III) complex (**1**) with \mathbf{HLCI} are reported.

EXPERIMENTAL

Materials and methods

2-Acetylpyridine ($\geq 99\%$) and Girard's T reagent (99 %) were obtained from Aldrich. The IR spectra were recorded in the region 4000–400 cm^{-1} on a Nicolet 6700 FT-IR spectrometer using the ATR technique (*vs* – very strong, *s* – strong, *m* – medium, *w* – weak, *bs* – broad signal). ^1H - and ^{13}C -NMR spectra of ligand \mathbf{HLCI} were recorded on Bruker Avance Ultrashield 500 plus spectrometer (^1H at 500 MHz; ^{13}C at 125 MHz) at room temperature using TMS as the internal standard in $\text{DMSO}-d_6$. Elemental analyses (C, H and N) were performed by standard micro-methods using an Elementar Vario ELIII C.H.N.S.O analyzer.

Magnetic properties of a polygrain sample were investigated using a Quantum Design MPMS-XL-5 SQUID magnetometer. The susceptibility was measured between 2 K and 300 K in a constant magnetic field of 1 kOe*. All the presented data are corrected for the tempera-

* 1 Oe = 79.57747 A/m

ture independent diamagnetic contribution of the sample holder and the inner shell electrons according to the Pascal tables.⁸

Synthesis of ligand HLCI, (E)-N,N,N-trimethyl-2-oxo-2-(2-(1-(pyridin-2-yl)ethylidene)hydrazinyl)ethan-1-aminium chloride

The ligand **HLCI** was synthesized in the reaction of 2-acetylpyridine (1.67 g, 1.00 mmol) and Girard's T reagent (1.12 mL, 1.00 mmol) in methanol (50 mL) as described previously.⁶ The reaction mixture was acidified with 3–4 drops of 2 M HCl and refluxed for 120 min at 85 °C.

The characterization data for **HLCI** are given in the Supplementary material to this paper. Signals of two rotational isomers of the hydrazone tautomeric form with the *E* configuration (ratio 1:0.4) were observed in the NMR spectra of ligand **HLCI**.⁶

*Synthesis of the Fe(III) complex (**I**)*

Ligand **HLCI** (70.5 mg, 0.30 mmol) was dissolved in methanol (20 mL) and then a solution of Fe(NO₃)₃·9H₂O (121 mg, 0.33 mmol) in H₂O (5 mL) and a solution of NH₄SCN (60 mg, 0.90 mmol) in H₂O (5 mL) were added. The reaction mixture was stirred with heating for 3 h at 65 °C. Dark red crystals suitable for X-ray analysis arose from the reaction solution after slow evaporation of the solvent in a refrigerator (\approx 7 °C) during two weeks.

X-Ray crystallography

The molecular structure of complex **I** was determined by the single-crystal X-ray diffraction method. The intensity data were collected at room temperature with a Bruker-Nonius KappaCCD diffractometer using graphite-monochromated MoK α radiation ($\lambda = 0.71073 \text{ \AA}$). Data reduction and cell refinement were performed using DENZO and SCALEPACK.⁹ The structure was solved using the WINGX¹⁰ package by direct methods (SIR-92¹¹) and refined by least-squares against F^2 (SHELX-2016¹²). All non-hydrogen atoms were refined anisotropically, while the hydrogen atoms were included in the model at the geometrically calculated positions and refined using a riding model.

The results of the crystal structure analysis for **I** are given in the Supplementary material to this paper.

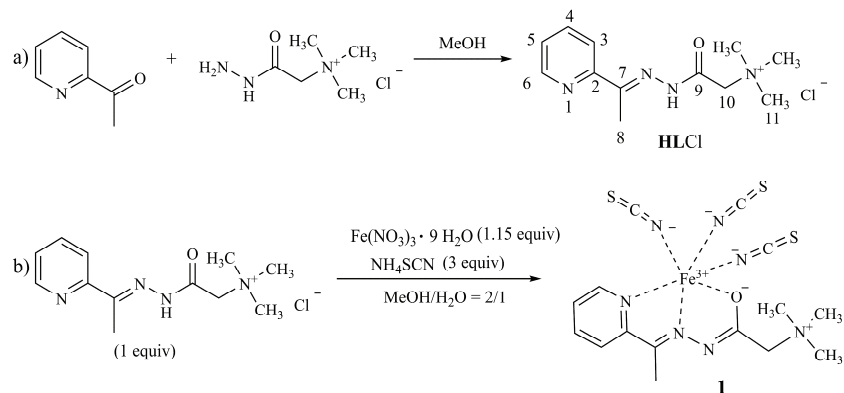
Antimicrobial activity

The antimicrobial activity of tested compounds was investigated against six different laboratory control strains of bacteria, *i.e.*, *Staphylococcus aureus* (ATCC 6538), *Bacillus subtilis* (ATCC 6633), *Escherichia coli* (ATCC 8739), *Klebsiella pneumoniae* (ATCC 13883), *Salmonella enterica* subsp. *enterica* serovar *Typhimurium* (ATCC 14028) and *Pseudomonas aeruginosa* (ATCC 9027), and one strain of yeast *Candida albicans* (ATCC 10231). In order to determine the minimum inhibitory concentrations (*MIC*) of the prepared samples, a broth microdilution method was used. The *MIC* values were determined according to Clinical and Laboratory Standards Institute (CLSI 2016). The assay was performed in 96-well microtiter plates with test strains suspended in Müller-Hinton and Sabouraud broth for the bacteria and yeast, respectively. The final concentration of each bacterial strain was adjusted to 2×10^6 and $2 \times 10^5 \text{ CFU mL}^{-1}$ for the *C. albicans*. Triphenyltetrazolium chloride (TTC, Aldrich, USA) was added to the culture medium as growth indicator. The wells containing only microorganisms and TTC were used as positive control of growth. Bacterial growth was determined after 24 h, while growth of *C. albicans* was determined after 48 h of incubation at 37 °C. The *MIC* determinations were performed in duplicate, and reference antimicrobial drugs meropenem, amikacin, and amphotericin B (Sigma-Aldrich) were included in the test.

RESULTS AND DISCUSSION

Synthesis

The ligand (*E*)-*N,N,N*-trimethyl-2-oxo-2-(2-(1-(pyridin-2-yl)ethylidene)hydrazinyl)ethan-1-aminium chloride (**HLCI**), was obtained in the condensation reaction of 2-acetylpyridine and Girard's T reagent in methanol, Scheme 1a.⁶ Reaction of the ligand **HLCI** with $\text{Fe}(\text{NO}_3)_3 \cdot 9\text{H}_2\text{O}$ and NH_4SCN in mole ratio 1:1.15:3 in methanol/water mixture resulted in the formation of mononuclear isothiocyanato Fe(III) complex (**1**) with composition $[\text{FeL}(\text{NCS})_3]$, Scheme 1b. In complex **1**, Fe(III) is hexacoordinated with the pyridine nitrogen, azomethine nitrogen and carbonyl oxygen atoms from the deprotonated hydrazone ligand and three thiocyanate ligands coordinated through nitrogen atoms.



Scheme 1. Synthesis of: a) ligand **HLCI** and b) complex **1**.

IR Spectroscopy

In the IR spectrum of complex **1**, a band at 1620 cm^{-1} corresponding to the $\nu(-\text{O}-\text{C}=\text{N})$ vibration of deprotonated α -oxyazine form of the ligand appeared instead of the carbonyl group band of noncoordinated **HLCI** at 1700 cm^{-1} . The coordination of azomethine nitrogen results in shift of $\nu(\text{C}=\text{N})$ from 1612 cm^{-1} in the spectrum of **HLCI** to 1598 cm^{-1} in the spectrum of complex **1**.

In the spectrum of complex **1**, strong bands at 2036 and 2024 cm^{-1} could be attributed to the SCN^- groups coordinated in meridional alignment through the nitrogen atom.¹³

*Crystal structure of **1***

The molecular structure of **1** is shown in Fig. 1. Selected bond distances and angles are given in Table I. Two nitrogen atoms (N1 and N2) and one oxygen atom (O1) of the tridentate ligand **L** in combination with three nitrogen atoms (N5, N6 and N7) of three thiocyanate ligands in a meridional alignment complete

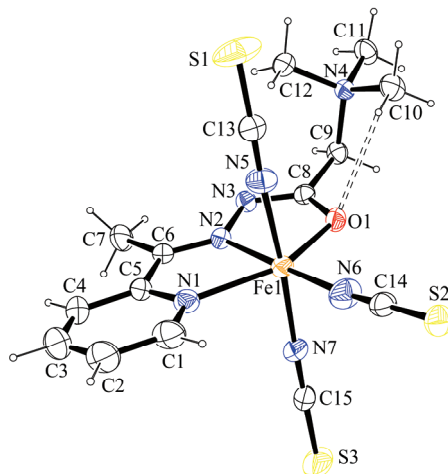


Fig. 1. The ORTEP drawing of complex **1**. Dashed line represents C–H \cdots O hydrogen bond. Thermal ellipsoids are drawn at the 30 % probability level.

the octahedral coordination of the iron(III) ion. The tridentate NNO coordination of ligand **L** to Fe(III) ion generates two fused five-membered chelation rings (Fe–N–C–C–N and Fe–N–N–C–O) that are non-coplanar. The dihedral angle between chelate rings (Fe–N–C–C–N and Fe–N–N–C–O) is 3.8°. The maximum deviation from the average ring skeleton including the metal sums 0.07 Å. The Fe(III) ion in **1** is more tied to the imine nitrogen atom of the ligand **L** than to the pyridine nitrogen atom, as indicated by the Fe1–N2, 2.109(3) Å and Fe1–N1, 2.149(3) Å bond lengths (Table I). The Fe–N_{py} (Fe1–N₁, 2.149(3) Å) bond distance is slightly shorter than the mean bond distance (2.167 Å) observed in two crystallographically independent complex units present in the crystal structure of analogous [FeL₂Cl₃]¹⁴ complex (were L₂ is the condensation product of 2-formylpyridine and Girard's T reagent). However, Fe–N_{imine} (Fe1–N2, 2.109(3) Å) and Fe–O_{enolate} (Fe1–O1, 2.012(2) Å) bond distances are comparable to those observed in the reported [FeL₂Cl₃]¹⁴ complex. One of the measures of the octahedral strain is average ΔO_h value, defined as the mean deviation of 12 octahedral angles from ideal 90°. The distorted octahedron formed around Fe1 in **1** exhibits average ΔO_h value of 6.2°. The *trans* bond angles vary from 148.50(10) to 178.75(12)°. The N(CH₃)₃ group can occupy different positions to the rest of molecule by rotating around the C8–C9 and C9–N4 bonds. The orientation of N(CH₃)₃ can be described by the dihedral angle N4–C9–C8–N3 which amounts 98.5(3)°. The distance of the N4 atom from the mean coordination plane (Fe1,N1,N2,O1,N6) is 1.879(3) Å. The present orientation of the N(CH₃)₃ group is mostly determined by an intramolecular weak hydrogen bond C10–H10A \cdots O1 (Fig. 1, Table II) and C12–H12C \cdots π (chelate ring Fe–N–N–C–O) contact (Table III). The N-coordinated SCN[−] ligands are slightly bent, with the Fe–N–C bond angles varying from 171.5(4) to 174.1(3)° (Table I).

TABLE I. Selected bond lengths and bond angles for **1**

Selected bond lengths, Å			
Fe1–N6	1.981(4)	N2–N3	1.391(4)
Fe1–O1	2.012(2)	N5–C13	1.136(5)
Fe1–N7	2.035(3)	N6–C14	1.154(5)
Fe1–N5	2.041(3)	N7–C15	1.149(5)
Fe1–N2	2.109(3)	N2–C6	1.282(4)
Fe1–N1	2.149(3)	N3–C8	1.308(4)
S1–C13	1.594(4)	O1–C8	1.287(4)
S2–C14	1.612(4)		
S3–C15	1.608(4)		
Selected bond angles, °			
N6–Fe1–O1	104.43(13)	N5–C13–S1	178.8(4)
N6–Fe1–N7	90.74(14)	N6–C14–S2	179.3(4)
O1–Fe1–N7	93.25(12)	N7–C15–S3	178.8(5)
N6–Fe1–N5	91.08(15)	C13–N5–Fe1	171.5(4)
O1–Fe1–N5	89.55(12)	C14–N6–Fe1	173.2(3)
N7–Fe1–N5	176.18(13)	C15–N7–Fe1	174.1(3)
N6–Fe1–N2	178.75(12)		
O1–Fe1–N2	74.82(9)		
N7–Fe1–N2	90.31(12)		
N5–Fe1–N2	87.91(12)		
N6–Fe1–N1	107.04(15)		
O1–Fe1–N1	148.50(10)		
N7–Fe1–N1	87.83(12)		
N5–Fe1–N1	88.43(13)		
N2–Fe1–N1	73.69(11)		

As shown in Fig. 2, weak intermolecular interactions are present in the crystal packing of **1**, *i.e.*, $\pi\cdots\pi$ interactions,¹⁵ non-classical hydrogen bonds (C–H \cdots O and C–H \cdots S)¹⁶ and C–H \cdots π (pyridine ring). The complex molecules [FeL(NCS)₃] connected by C–H \cdots O and C–H \cdots S hydrogen bonds formed around the inversion centres at $\frac{1}{2}$ 0 $\frac{1}{2}$ and 0 0 $\frac{1}{2}$, respectively, generate zigzag chains parallel with the [100] direction (Fig. 2, Table II). In the crystals of **1**, the $\pi\cdots\pi$ and C–H \cdots π (pyridine ring) interactions (Fig. 2, Table III) serve to connect neighbouring hydrogen-bonded chains into 2D layers parallel with the (010) lattice plane. Furthermore, the layers are connected by intermolecular hydrogen bond between aromatic carbon atom C2 and S2 at $-x$, 1–y, 2–z. Crystallographic programs ORTEP-3 for Windows¹⁷ and Mercury¹⁸ were used to prepare the drawings.

Magnetic properties of complex **1**

The susceptibility (Fig. 3) follows the Curie–Weiss law $\chi = C/(T-\theta)$, with a Curie constant $C = 4.29$ emu* K mol⁻¹ and a Curie–Weiss temperature $\theta = -0.9$ K.

* 1 emu = 10⁻³ A m²

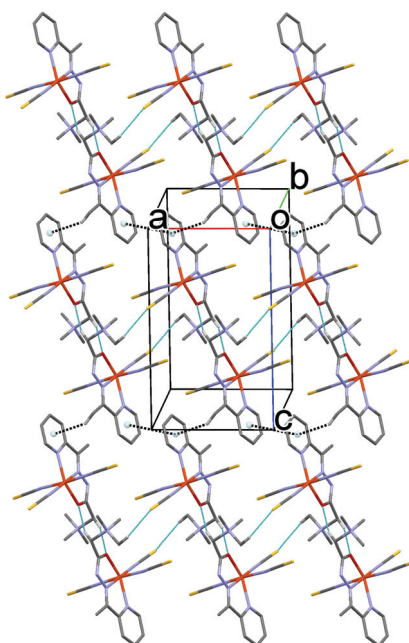


Fig. 2. Perspective view of the 2D assembly of complex **1** parallel with (010) generated by C–H···O and C–H···S hydrogen bonds and $\pi\cdots\pi$ and C–H··· π (pyridine ring) interactions. Hydrogen atoms have been omitted for the sake of clarity except those involved in the intermolecular interactions.

TABLE II. Hydrogen-bond parameters for complex **1**

D–H···A	D–H bond length, Å	H···A distance, Å	D···A distance, Å	$\angle D\text{--H}\cdots A$, °	Symmetry operation on A
C9–H9B···O1	0.97	2.57	3.504(4)	163	$1-x, -y, 1-z$
C12–H12B···S2	0.96	2.84	3.776(4)	165	$-x, -y, 1-z$
C2–H2···S2 inter layer	0.93	2.88	3.767(4)	160	$-x, 1-y, 2-z$
Intra C10–H10A···O1	0.96	2.53	3.105(5)	119	
Intra C7–H7A···N3	0.96	2.46	2.866(5)	105	

The fit is shown as the full green line in Fig. 3. The effective magnetic moment per Fe(III) can be calculated as $\mu_{\text{eff}} = 5.9 \mu_B$.¹⁹ This value is in excellent agreement with the theoretically predicted value for Fe(III) ion with a ground state term $^6S_{5/2}$ with no orbital angular momentum.²⁰

The temperature dependent effective magnetic moment is shown in the inset in Fig. 3. From room temperature down to approximately 20 K, the value remains constant at $\approx 5.9 \mu_B$, which is in agreement with the value obtained from the Curie constant. Below 20 K, the effective magnetic moment slightly decreases from 5.9 to 4.7 μ_B at the lowest temperature of 2 K. This small decrease in the effective magnetic moment and the associated deviation of the temperature dependent susceptibility from a perfect Curie law $1/T$, is responsible for the obtained small negative value of the Curie–Weiss temperature of –0.9 K.

The decrease of effective magnetic moment at low temperatures could in principle be the result of at least three different terms in the magnetic Hamil-

tonian,²¹ *i.e.*, a) a weak antiferromagnetic interaction between the Fe(III) magnetic moments, b) spin-orbit coupling and c) a crystal field effect.

TABLE III. The geometrical parameters describing π - π and C–H \cdots π (ring) interactions in **1**; Cg(I) and Cg(J) are centroids of rings (I) and (J), respectively. Labels of rings: (1) = N(1), C(1)–C(5); (2) = Fe1–O1–C8–N3–N2

Cg(I)	Cg(J)	Cg(I)–Cg(J) distance, Å	\angle between ring (I) and ring (J) planes °	\angle between Cg(I)Cg(J) vector and normal to ring (I), °	\angle between Cg(I)Cg(J) vector and normal to ring (J), °	Distance between Cg(I) and normal projection of Cg(J) on ring (I), Å	Sym- metry code on ring J
Cg(I1)	Cg(J1)	4.003(3)	0.0(2)	23.2	23.2	1.576	$-x, -y,$ $2-z$
C–H	Cg(J)	H \cdots Cg(J) distance, Å	Perpen- dicular distance of H to ring (J), Å	\angle C– H \cdots Cg(J), °	\angle between H–Cg line and perpen- dicular H- -ring-plane line, °		
C7–H7C	Cg(1)	2.89	2.89	145	2.85		$1-x, -y,$ $2-z$
C12–H12C (Intra)	Cg(2)	2.98	–2.62	117	28.48		

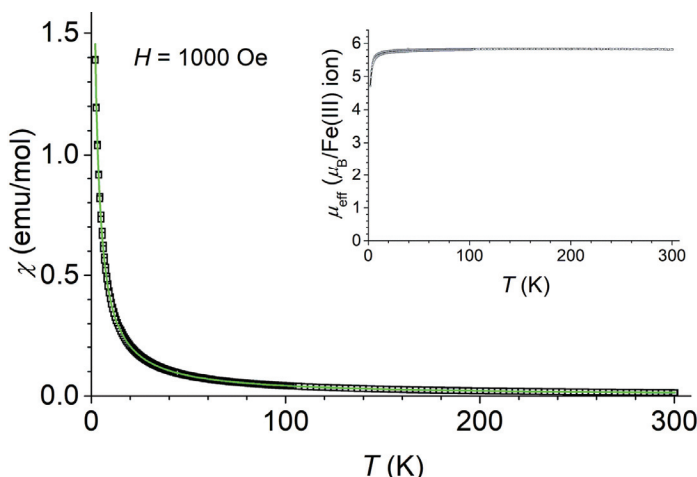


Fig. 3. Temperature dependence of the susceptibility. The full (green, electronic version of the paper) line is a fit with the Curie–Weiss law with parameters as described in the text. Inset: temperature variation of effective magnetic moment per Fe(III) ion.

As the distances between the nearest neighbour Fe(III) ions are as large as 7.7594(9) Å, a considerable magnetic interaction between them is very unlikely,

and hence the first (a) possibility can be ruled out. Moreover, the measured effective magnetic moment is in excellent agreement with the spin only contribution ($J = S = 5/2$, $L = 0$) and thus, the second (b) possibility can also be ruled out. Hence, a small temperature dependence of effective magnetic moment may be attributed to a crystal field effect.

Antimicrobial activity

The investigated compounds **HLC1** ligand and complex **1** were inactive against almost all the tested microbial strains, Table S-I of the Supplementary material. Very low activity of complex **1** ($MIC = 500 \mu\text{g mL}^{-1}$) was observed against *C. albicans*. $\text{Fe}(\text{NO}_3)_3 \cdot 9\text{H}_2\text{O}$ and NH_4SCN were inactive against all the investigated microbial strains. Antimicrobial activity of complex **1** is significantly lower than those of the previously reported $[\text{FeL}^1(\text{NCS})_2]\text{SCN} \cdot 2\text{H}_2\text{O}$ and $[\text{FeL}^1(\text{NCS})_2]_2[\text{Fe}(\text{H}_2\text{O})(\text{NCS})_5] \cdot 4\text{H}_2\text{O}$ complexes. Some explanation for such results are the differences in charge, geometry and stability in solution between complex **1** and $[\text{FeL}^1(\text{NCS})_2]\text{SCN} \cdot 2\text{H}_2\text{O}$ and $[\text{FeL}^1(\text{NCS})_2]_2[\text{Fe}(\text{H}_2\text{O})(\text{NCS})_5] \cdot 4\text{H}_2\text{O}$.⁷

CONCLUSIONS

The reaction of condensation product of 2-acetylpyridine and Girard's T reagent with $\text{Fe}(\text{NO}_3)_3 \cdot 9\text{H}_2\text{O}$ and NH_4SCN gives a mononuclear Fe(III) complex. The octahedral geometry of the neutral Fe(III) complex consists of a pyridine nitrogen, an azomethine nitrogen and carbonyl oxygen atoms from the deprotonated hydrazone ligand and three isothiocyanato ligands. The measured effective magnetic moment for the Fe(III) complex, $\mu_{\text{eff}} = 5.9 \mu_B$, corresponds to Fe(III) ion with the ground state term ${}^6\text{S}_{5/2}$ without orbital angular momentum. The hydrazone ligand and its Fe(III) complex showed negligible activity against the tested microbial strains.

SUPPLEMENTARY MATERIAL

The additional data are available electronically at the pages of journal website: <http://www.shd.org.rs/JSCS/>, or from the corresponding author on request.

Additional crystallographic data for the structure reported in this paper have been deposited at the Cambridge Crystallographic Data Centre with quotation number CCDC 1863722 and is available free of charge on request via www.ccdc.cam.ac.uk/data_request/cif.

Acknowledgements. The Ministry of Education, Science and Technological development of the Republic of Serbia (Grant OI 172055) and Slovenian Research Agency (P-0175 and P2-0348) supported this work.

ИЗВОД

СИНТЕЗА, КАРАКТЕРИЗАЦИЈА И АНТИМИКРОБНА АКТИВНОСТ ИЗОТИОЦИЈАНОТО
КОМПЛЕКСА Fe(III) ЖИРАРОВОГ РЕАГЕНСА СА Т ХИДРАЗОНОМ

БОЖИДАР ЧОБЕЉИЋ¹, ANDREJ PEVEC², ЗВОНКО ЈАГЛИЧИЋ³, МИЛИЦА Р. МИЛЕНКОВИЋ¹, IZTOK TUREL²,
ДУШАНКА РАДАНОВИЋ⁴, МАРИНА МИЛЕНКОВИЋ⁵ и КАТАРИНА АНЂЕЛКОВИЋ¹

¹Хемијски факултет у Београду, Студентски трг 12–16, Београд, ²Faculty of Chemistry and Chemical Technology, University of Ljubljana, Večna pot 113, 1000 Ljubljana, Slovenia, ³Institute of Mathematics, Physics and Mechanics & Faculty of Civil and Geodetic Engineering, University of Ljubljana, Jadranska 19, Ljubljana, Slovenia, ⁴Институт за хемију, технолоџију и међалургију, Универзитет у Београду, Његошева 12, Ј.п.р. 11000 Београд и ⁵Фармацеутски факултет, Катедра за микробиологију и имунологију, Универзитет у Београду, Војводе Степе 450, 11221 Београд

Изотиоцијанато комплекс Fe(III) са (E)-N,N,N-тритметил-2-оксо-2-(1-(пиридин-2-ил)етилиден)хидразинил)етан-1-аминијум лигандром је синтетисан и охарактерисан елементалном анализом, IC спектроскопијом и ренгенском структурном анализом. Октаедарску геометрију Fe(III) комплекса чине хидразонски лигандр координован у депротонованој форми преко пиридинског азота, азометинског азота и карбонилног кисеоника и три изотиоцијанато лиганда на преосталим координационим местима. Измерени ефективни магнетни момент за Fe(III) комплекс одговара високоспинском Fe(III). Хидразонски лигандр и његов Fe(III) комплекс показују мању активност на испитане сојеве микроорганизама него стандардни антимикробни лекови.

(Примљено 28. августа, ревидирано и прихваћено 19. септембра 2018)

REFERENCES

1. L. N. Suvarapu, Y. K. Seo, S. O. Baek, V. R. Ammireddy, *Eur. J. Chem.* **9** (2012) 1288
2. Lj. S. Vojinović-Jesić, S. B. Novaković, V. M. Leovac, V. I. Češljević, *J. Serb. Chem. Soc.* **77** (2012) 1129
3. B. Čobeljić, M. Milenković, A. Pevec, I. Turel, M. Vujčić, B. Janović, N. Gligorijević, D. Sladić, S. Radulović, K. Jovanović, K. Andđelković, *J. Biol. Inorg. Chem.* **21** (2016) 145
4. M. R. Milenković, B. Čobeljić, K. Andđelković, I. Turel, *Eur. J. Inorg. Chem.* **2018** (2018) 838
5. B. Čobeljić, A. Pevec, S. Stepanović, V. Spasojević, M. Milenković, I. Turel, M. Swart, M. Gruden-Pavlović, K. Adaila, K. Andđelković, *Polyhedron* **89** (2015) 271
6. B. Čobeljić, A. Pevec, S. Stepanović, M. R. Milenković, I. Turel, M. Gruden, D. Radanović, K. Andđelković, *Struct. Chem.* **29** (2018) 1797
7. K. Andđelković, M. R. Milenković, A. Pevec, I. Turel, I. Z. Matić, M. Vujčić, D. Sladić, D. Radanović, G. Brađan, S. Belošević, B. Čobeljić, *J. Inorg. Biochem.* **174** (2017) 137
8. O. Kahn, *Molecular Magnetism*, VCH Publishing, Weinheim, 1993, p. 2
9. Z. Otwinowsky, W. Minor, *Methods Enzymol.* **276** (1997) 307
10. L. J. Farrugia, *J. Appl. Crystallogr.* **32** (1999) 837
11. A. Altomare, G. Cascarano, C. Giacovazzo, A. Guagliardi, *J. Appl. Crystallogr.* **26** (1993) 343
12. G. M. Sheldrick, *Acta Crystallogr., C* **71** (2015) 3
13. K. Nakamoto, *Infrared and Raman Spectra of Inorganic and Coordination Compounds*, 4th ed., Wiley-Interscience, New York, 1986, p. 283
14. O. V. Palamarciuc, P. N. Bourosh, M. D. Revenco, J. Lipkowski, Y. A. Simonov, R. Clérac, *Inorg. Chim. Acta* **363** (2010) 2561
15. C. Janiak, *J. Chem. Soc., Dalton Trans.* (2000) 3885
16. T. Steiner, *Angew. Chem. Int. Ed.* **41** (2002) 48

17. L. J. Farrugia, *J. Appl. Crystallogr.* **45** (2012) 849
18. C. F. Macrae, P. R. Edgington, P. McCabe, E. Pidcock, G. P. Shields, R. Taylor, M. Towler, J. van de Streek, *J. Appl. Crystallogr.* **39** (2006) 453
19. F. E. Mabbs, D. J. Machin, *Magnetism and Transition Metal Complexes*, Dover Publications, Mineola, New York, 1973
20. N. W. Ashcroft, N. D. Mermin, *Solid State Physics*, Saunders College Publishing, Philadelphia, PA, 1976
21. J. M. D. Coey, *Magnetism and magnetic materials*, Cambridge University Press, New York, 2010.